ISSN 1330–0008
CODEN FIZAE4

TEMPERATURE DEPENDENCE OF THE CROSS SECTION σ_{5S} FOR THE ENERGY POOLING PROCESS Na(3P) + Na(3P) → Na(5S) + Na(3S)

VLASTA HORVATIĆ

Institute of Physics, Bijenička 46, HR-10000 Zagreb, Croatia
E-mail address: blecic@ifs.hr

Received 18 September 2003; revised manuscript received 6 October 2003
Accepted 13 October 2003 Online 19 April 2004

Applying the method of laser induced fluorescence, the cross section σ_{5S} for the energy pooling process Na(3P) + Na(3P) → Na(5S) + Na(3S) has been determined at temperatures in the interval from 567 to 676 K. It has been found that σ_{5S} decreases with increasing temperature, exhibiting $\sigma_{5S} \propto T^{-1.3}$ dependence. The results show excellent agreement with the recent theoretical calculations. Also, the determined temperature dependence of the cross section σ_{5S} fits very well into recently reported general σ vs. T scheme for the exothermic collisional excitation energy transfer cross sections, which includes various collision partners and various types of collisional excitation energy transfer processes with different energy defects.

PACS numbers: 31.70.Hq, 34.50.-s, 34.50.Rk UDC 535.353

Keywords: energy pooling process, Na(3P) + Na(3P) → Na(5S) + Na(3S), laser induced fluorescence, collisional excitation energy transfer, cross section

1. Introduction

Collisional excitation energy transfer (CEET) in thermal collisions between excited atoms and molecules in gases has been the subject of numerous investigations during the last decades. The CEET processes are important mechanisms for establishing the population distributions, and very often play a crucial role in many phenomena in excited gaseous media. Studies of such interactions are of great interest in a variety of fields, both fundamental and applied.

The cross sections for CEET processes occurring in excited pure or mixed alkali vapours constitute a vast majority of the body of the CEET cross sections data published so far. The review paper of Krause [1] summarized the most relevant

experimental and theoretical results in this area published until 1975. The extensive list of more recent references pertaining to this subject can be found in Refs. [2] and [3]. Alkalis owe their popularity to the relative simplicity they offer to experimental and theoretical treatment. Nevertheless, the discrepancies between theoretical and experimental results, as well as among experimental results of different authors for the same CEET process, are frequent.

In any situation where the data are numerous and apparent regularities among them are few, it is very helpful if a new systematic behaviour with respect to a given common characteristic parameter can be discerned. That can inspire new theoretical approaches and interpretations, eventually leading to a better understanding of the nature of these important physical processes.

Since the earliest CEET investigations [1] until recently [4], the relationship $\sigma \propto 1/\Delta E$ between exothermic cross sections σ and the energy defect ΔE of CEET in homonuclear and heteronuclear alkali – alkali collisions has been repeatedly noticed, but an adequate, general theoretical description of this phenomenon is still lacking.

Quite recently the regularity, so far unnoticed, in temperature behaviour of the cross sections for exothermic CEET processes has been reported [3]. Namely, depending on the magnitude of the cross section, the slope of the $\sigma(T)$ curves in the log–log diagram continuously changes from approximately 2 to -1.5 with increasing the cross section value. This regularity holds regardless of the type of collision partners, the kind of CEET process or the value of energy defect involved, meaning that that neither the energy defect nor the type of interaction, but only the absolute magnitude of the thermal cross sections governs the thermal cross section temperature behaviour. Semi-empirically determined regularities in behaviour, like the one just mentioned, can be very useful for experimentalists in estimating the cross-section values if there is a lack of relevant data.

The body of experimental cross-section data available in literature is huge, but most frequently the reported values were measured at single temperature or in a very narrow temperature range where in particular experiment the relevant signals could be measured. Unfortunately, there are very few papers [5–7] that report quasi-continuous measurements of the cross section – temperature dependence. Such measurements are very valuable because the obtained results can provide not only information about the cross section values corresponding to temperatures at which the measurements are hard or impossible to perform, but also the more complete insight into physics that lies behind.

The investigation presented in this paper belongs to this rare type of measurements and contributes to the pool of data on continuously slope-varying $\sigma(T)$ curves [3] for exothermic CEET processes with the results for the temperature dependence of the cross section σ_{5S} for the exothermic energy pooling reaction in sodium

$$\mathrm{Na(3P) + Na(3P) \quad \rightarrow \quad Na(5S) + Na(3S).} \tag{1}$$

The observation of the above process was reported in 1976 by Allegrini et al. [8]. The first quantitative measurements were due to Kushawaha and Levental [9], who found $\sigma_{5S} \approx 7.5 \cdot 10^{-20}$ cm^2 to be practically constant in the temperature range be-

tween 465 and 510 K. The measurements in Ref. [9] were burdened with radiation trapping effects and some difficulties in the determination of the spatial distribution and absolute value of the density of excited atoms. In 1983 Huennekens and Gallagher [10] and Allegrini et al. [11] re-measured this cross section in the experiments, which rigorously took care of the sources of errors that caused difficulties in the former experiment. They obtained the following cross section values: $(32 \pm 11) \cdot 10^{-16}$ cm^2 at 600 K [10] and $(40 \pm 14) \cdot 10^{-16}$ cm^2 at 483 K [11]. Both cited values for σ_{5S} are by a factor two greater than the values originally published, in order to properly account for the number of atom pairs in a cell, as pointed out by Bezuglov et al. [12].

Theoretical calculations of the σ_{5S} cross section were performed by several authors [13–17]. All calculations predict mild decrease in the cross section value with increasing temperature. As for the absolute values, the cross sections reported in Refs. [13–16] are all systematically smaller (by 60 % to a factor of three) than the experimental values measured by authors of Refs. [10] and [11], while recent values obtained by Yurova [17] show excellent agreement (differences amount to 15 % at most) with the experimental data. The calculations in Ref. [17] differ from all previous calculations [13–16] by inclusion of the fine-structure effects in the computation. The necessity of doing that has been pointed out earlier [7,16], while the actual refinement of the calculations in that respect favourably affected the agreement between theory and experiment.

The experiment presented here is the continuation of the previous work [7] which yielded the temperature dependence of the cross section for another well known energy pooling process in sodium, i.e. Na(3P) + Na(3P) → Na(4D) + Na(3S). The measurements of σ_{5S} cover the temperature interval from 567 to 676 K. Sodium atoms were excited to the 3P state by cw laser radiation, while the quantities required to obtain the cross section (relative populations of the 3P and 5S levels, spatial distribution of the number density of the Na atoms in the 3P state and sodium ground-state density) were determined by a combination of the fluorescence and laser absorption measurements. The measurement method applied [18] does not require the knowledge about the effective lifetime of the 3P state, which is advantageous in the presence of substantially trapped Na resonance radiation at the investigated temperatures, and eliminates the trapping as a source of possible systematic error. The cross section σ_{5S} has been found to decrease with increasing temperature as $\sigma_{5S} \propto T^{-1.3}$. The cross section value obtained at $T = 600$ K and the value predicted by $\sigma_{5S}(T)$ dependence at $T = 483$ K are in excellent agreement with the results reported in Refs. [10] and [11], respectively.

2. Experiment

2.1. Experimental details

The results presented in this paper for the temperature dependence of the cross section σ_{5S} of the process (1), have been obtained using the experimental arrange-

ment and the procedure described in a preceding paper [7] on 4D-energy-pooling in sodium, and all experimental details can be found there. For the readers' convenience, the relevant particularities will be repeated.

The sodium vapours were created in a resistively heated, T-shaped stainless-steal heat-pipe oven with Pyrex glass windows, which was not running in the heat-pipe mode. Argon was used as the buffer gas. The length of the vapour column was $L = (7 \pm 1)$ cm.

The excitation of sodium atoms was done by the laser (Spectra Physics system: Ar-ion laser model 2020 + a single-mode, frequency stabilised ring-dye laser model 380 D with Rh6G dye) tuned to the red wing of the D1 line. Detunings from the line centre were typically $\Delta\lambda_L = \lambda_L - \lambda_{1/2} \approx 0.01 - 0.4$ nm. The central part of the collimated dye-laser beam (diameter: 4 mm), having nearly homogeneous power distribution was used for the excitation. The maximum laser power just in front of the heat-pipe entrance window was chosen so as to optimize the signals at the particular investigated temperature, and the typical values were between 90 and 120 mW.

The pump beam was shone through the heat-pipe (z-direction), and the fluorescence was monitored through the heat pipe side arm at right angles (y-direction) to the laser beam propagation direction. The optical path for the fluorescence radiation was $d \approx L/4$. The fluorescence was analysed by a 1 m McPherson monochromator supplied with a RCA C31034A photomultiplier. The length of the central part of the cylindrical fluorescence zone that was imaged in 1 : 2 ratio onto the entrance slit of the monochromator was about 1 cm. With the slit-widths of 100 μm, the band-pass of the monochromator was 0.1 nm. The monochromator slits were parallel to the fluorescence zone axis (z-direction) and, with the 100 μm-slits, the monitored volume of the fluorescence zone was the central slab having the thickness $\Delta x = 0.02$ cm. The spectral response of the detection system was measured using a calibrated W2KGV22i tungsten-ribbon lamp.

Typical measurement sequence at each investigated temperature involved recording of the fluorescence signals of the resonant doublet and energy pooling line by scanning the monochromator across the 3P $\rightarrow$ 3S and 5S $\rightarrow$ 3P transitions, and measurements of the spatial distribution of the $3P_{3/2}$ population number density, while the pump laser was kept locked at a chosen frequency $\nu_L = \nu_{1/2} - \Delta\nu_L$ in the red wing of the Na D1 line.

From the general features of the fluorescence radiation, it follows that the relaxation of the collisionally populated states will result in an isotropic an unpolarized emission, while the direct fluorescence due to the optical excitation by a linearly polarised laser is expected to be polarized and anisotropic. In particular, the direct fluorescence of the D2 line at $J = 3/2 \rightarrow J = 1/2$ transition exhibits pronounced polarization anisotropy, while the direct fluorescence of the D1 line is always spatially isotropic because it emerges at the transition between two levels with the same total angular momentum $J = 1/2$. In the present experiment the line that was excited by the laser was D1 line, and the emitted direct fluorescence was isotropic. The fluorescence of the D2 line was also isotropic because $3P_{3/2}$ state was popu-

lated by collisional excitation transfer. The latter is valid also for the fluorescence of energy-pooling line. There were also no problems regarding the laser-scattered light because the fluorescence of interest was always monitored at the wavelengths which differed from the laser wavelength by at least 1 nm.

The population of the $3P_{3/2}$ state was determined by laser absorption measurement. The diode-laser beam (single-mode, frequency stabilised ML 2701 diode, $\lambda = 831$ nm at 26^0 C, maximal power 8 mW), having 0.5 mm in diameter and the power of 5 μW, passed through the centre of the excitation zone, counter-propagating to the pump beam. The absorption along the path L was measured by scanning the diode laser across the $3P_{3/2} \rightarrow 3D_{3/2,5/2}$ transition at 819.7 nm, and the transmitted intensity was detected by a photodiode. The confocal Fabry–Perot interferometer (f.s.r. 2 GHz) was used to calibrate the dispersion of the spectrum. Under the experimental conditions realized, it was found that the contribution of the $3P_{3/2} \rightarrow 3D_{3/2}$ absorption to the peak absorption k_0 of the $3P_{3/2} \rightarrow 3D_{5/2}$ line was negligible [7], and therefore the average number density $\overline{N}_{3/2}$ in the Na($3P_{3/2}$) state along the path L was determined from the peak absorption coefficient of the measured spectrum.

The spatial distribution $N_{3/2}(r)$ of the atoms in the $3P_{3/2}$ state is radially symmetric as a consequence of the power profile of the pump laser beam, the excitation and the heat-pipe geometry. The $N_{3/2}(r)$ was measured by translating the diode-laser beam across the excitation zone diameter (x-direction) and parallel with its axis, while recording the corresponding absorption at the $3P_{3/2} \rightarrow 3D_{3/2,5/2}$ transition.

The Na ground-state number density N_{3S} was determined from the measurements of the absorption coefficient in the red quasistatic wing of the Na D1 line in the way previously described [7] and using the method reported in Ref. [19]. It was found that N_{3S} varied from $2.2 \cdot 10^{14}$ to $1.1 \cdot 10^{16}$ cm^{-3}. The error of the N_{3S} determination is ± 10 %, and it is mainly due to the uncertainty of the vapour column length L.

The temperature of the sodium vapour was determined in two ways. One way was to use the measured Na ground-state number density values and take the corresponding temperature from the vapour pressure curve [20]. The second way was to use the $3P_{3/2} \rightarrow 3D_{3/2,5/2}$ absorption spectra, and obtain the temperature by fitting the spectra with the sum of the two Doppler profiles [7]. The respective errors of the temperature determined in these two ways were ± 5 and ± 15 K, while the absolute values of the temperature agreed within mutual error bars. The temperature interval covered by the measurements was found to be between 567 and 676 K.

The experimentally determined temperatures were used to obtain the Maxwellian mean relative velocities $\overline{v}$ of the colliding sodium atoms. The error in $\overline{v}$ was estimated to be less than ± 2 % (at the actual temperatures in the experiment an uncertainty of ± 20 K accounts for the stated error).

2.2. Rate equation and the cross section evaluation formula

The transitions involved in the determination of the σ_{5S} cross section are indicated in the partial sodium term diagram shown in Fig. 1. Subsequent to the $Na(3S_{1/2}) \rightarrow Na(3P_{3/2})$ laser excitation, the Na(5S) state was populated due to

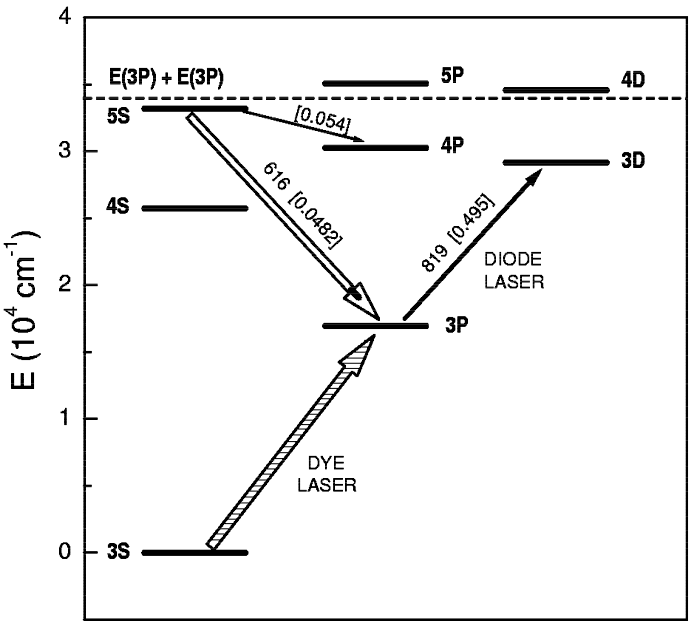

Fig. 1. Partial term diagram of sodium showing the energy levels relevant for the determination of the rate coefficient k_{5S} for the $Na(3P) + Na(3P) \rightarrow Na(5S) + Na(3S)$ *process. Sodium atoms in the* 3P *state were produced by dye-laser excitation in the red wing of the* D1 *line. The fluorescence signals were observed at the* $5S_{1/2} \rightarrow 3P_{3/2}$ *and* $3P_{1/2,3/2} \rightarrow 3S_{1/2}$ *transitions. The population in the* $3P_{3/2}$ *state was determined from absorption measurements by diode laser absorption at the* $3P_{3/2} \rightarrow 3D_{3/2,5/2}$ *transition. Numerical values represent the wavelengths in nanometers and the spontaneous emission coefficients in* $10^8\,s^{-1}$ *(in brackets) for the relevant transitions.*

Na(3P) + Na(3P) energy pooling collisions. The depopulation of the 5S level goes radiatively to the lower-lying P states, and collisionally by the back-energy-pooling process Na(5S) + Na(3S) → Na(3P) + Na(3P). The spontaneous emission rate for the 5S state is denoted by $A_{5S} = A_{5S\rightarrow 4P} + A_{5S\rightarrow 3P}$, while R_{5S}^{back} the labels the collisional relaxation rate to the Na(3P) level.

The steady-state, r-dependent population $N_{5S}(r)$ created under these conditions

is described by the following rate equation

$$\frac{\mathrm{d}N_{5\mathrm{S}}(r)}{\mathrm{d}t} = 0 = \frac{1}{2}k_{5\mathrm{S}}\big[N_{3\mathrm{P}}(r)\big]^2 - \big(A_{5\mathrm{S}} + R_{5\mathrm{S}}^{\mathrm{back}}\big)N_{5\mathrm{S}}(r), \tag{2}$$

where $k_{5\mathrm{S}}$ denotes the rate coefficient for the processes Na(3P) + Na(3P) → Na(5S) + Na(3S). The above equation holds for any r, and when applied to the centre of the excitation zone ($r = 0$), it yields the following solution for the rate coefficient $k_{5\mathrm{S}}$

$$k_{5\mathrm{S}} \quad = \quad \frac{2}{\big(1+\eta\big)^2}\frac{N_{5\mathrm{S}}^c}{(N_{3/2}^c)^2}\big(A_{5\mathrm{S}} + R_{5\mathrm{S}}^{\mathrm{back}}\big), \tag{3}$$

where superscript c indicates that the corresponding atom number densities are measured at the excitation zone axis, while $\eta = N_{1/2}^c/N_{3/2}^c$ with $N_{1/2}^c$ and $N_{3/2}^c$ denoting the populations of the fine structure levels of the 3P state.

The $N_{5\mathrm{S}}^c/(N_{3/2}^c)^2$ ratio was determined by measuring the respective fluorescence intensities I_{616} and $I_{3/2}(\Delta\nu)$ of the optically thin 616 nm line arising in the 5S → $3\mathrm{P}_{3/2}$ transition and the optically thin quasistatic blue wing of the sodium D2 line emitted at the detuning $\Delta\nu = \nu_{3/2} - \nu$ from the line centre.

The intensities of the emitted radiation are spectrally integrated over the frequencies within the band-pass $\delta\nu$ of the detection system. In the present experiment, the band-pass $\delta\nu = 0.1$ nm was large in comparison with the width of 616 nm line and I_{616} was spectrally integrated over the frequencies within the whole line profile. Therefore, the total fluorescence intensity of the 616 nm line emerging from the observation volume can be expressed as

$$I_{616} \quad \propto \quad h\nu_{616}A_{616}\int\limits_{\Delta V} N_{5\mathrm{S}}(x,y,z)\mathrm{d}x\mathrm{d}y\mathrm{d}z, \tag{4}$$

where $A_{616} = 4.82 \cdot 10^6$ s^{-1} according to Wiese et al. [21].

The $N_{5\mathrm{S}}(x,y,z)$ population density is independent of z (direction of propagation of the laser beam) and it can be also regarded independent of x along the segment Δx, because the width Δx of the thin volume slice observed by the monochromator is much smaller than the diameter of the excitation zone. Since $N_{5\mathrm{S}}(x,y,z)$ is apparently only a function of y, it can be expressed as $N_{5\mathrm{S}}(y) = N_{5\mathrm{S}}^c\mathcal{F}_{5\mathrm{S}}(y)$, where $N_{5\mathrm{S}}^c$ denotes population density at the excitation-zone axis and $\mathcal{F}_{5\mathrm{S}}(y)$ is the radial distribution function normalised to unity at $y = 0$. Thus, the expression for the I_{616} fluorescence intensity reads

$$I_{616} \quad \propto \quad h\nu_{616}A_{616}N_{5\mathrm{S}}^c\int\limits_{\Delta V} \mathcal{F}_{5\mathrm{S}}(y)\mathrm{d}y. \tag{5}$$

The spectral intensity of the optically-thin quasistatic blue wing of the sodium D2 line emitted at the detuning $\Delta\nu$ from the infinitesimal volume $\mathrm{d}V$ is given by:

$$\mathrm{d}I_{3/2}^{\nu}(\Delta\nu) \quad = \quad h\nu_{3/2}A_{3/2}^{\nu}\mathrm{d}\nu N_{3/2}(\Delta\nu,x,y,z)\mathrm{d}V, \tag{6}$$

where

$$A^{\nu}_{3/2} \quad = \quad 0.263\, N_{3\mathrm{S}} \frac{\mathcal{P}_{3/2}(Y)}{(\Delta\nu)^2} \tag{7}$$

is detuning-dependent spectral emission coefficient [7]. Relation (7) is applicable for the blue wing of the sodium D2 line and holds for the wing detunings $\Delta\nu \leq 3\Delta\nu_{\mathrm{fs}}$, where $\Delta\nu_{\mathrm{fs}}$ is the fine-structure splitting. In relation (7), $\mathcal{P}_{3/2}(Y)$ is a fourth-order polynomial in $Y = \Delta\nu/\Delta\nu_{\mathrm{fs}}$ which can be found in Ref. [7]. The polynomial $\mathcal{P}_{3/2}(Y)$ is a fit to the calculated theoretical absorption profile in the blue quasistatic wing of an alkali D2 line [7,22] that reproduces the calculated profile with an accuracy better than ± 0.5 %.

If the detuning $\Delta\nu = \nu_{3/2} - \nu$ from the line centre is large compared with band-pass $\delta\nu$ (fulfilled in the present experiment), the spectral emission coefficient $A^{\nu}_{3/2}$ can be regarded constant within the interval $(\nu, \nu + \delta\nu)$. The wing intensity $I_{3/2}(\Delta\nu)$ is due to a small portion of the $3\mathrm{P}_{3/2}$ state population radiating in the quasistatic wing at the frequency $\nu_{3/2} - \Delta\nu$, i.e. $N_{3/2}(\Delta\nu, x, y, z) \propto N_{3/2}(x, y, z) \exp\{-h\Delta\nu/(k_{\mathrm{B}}T)\}$, where $N_{3/2}(x, y, z)$ denotes the number density of the atoms radiating in the centre of the line. For the same reasons as in the case of $N_{5\mathrm{S}}(x, y, z)$, the $N_{3/2}(x, y, z)$ population density is only y-dependent, and can be expressed as $N_{3/2}(y) = N^{c}_{3/2}\mathcal{F}_{3/2}(y)$. Therefore, the emerging fluorescence intensity acquires the form

$$I_{3/2}(\Delta\nu) \quad \propto \quad h\nu_{3/2}A^{\nu}_{3/2}\delta\nu N^{c}_{3/2} \exp\{-h\Delta\nu/(k_{\mathrm{B}}T)\} \int\limits_{\Delta V} \mathcal{F}_{3/2}(y)\mathrm{d}y. \tag{8}$$

Intensities I_{616} and $I_{3/2}$ appearing in relations (5) and (8) are related to the measured ones by $I_{616}/I_{3/2} = I^{\mathrm{meas}}_{616}\zeta_{3/2}/(I^{\mathrm{meas}}_{3/2}\zeta_{616}) = 1.09\, I^{\mathrm{meas}}_{616}/I^{\mathrm{meas}}_{3/2}$, where ζ_{616} and $\zeta_{3/2}$ denote the spectral responses of the detection system at respective wavelengths.

The rate coefficients for forward and back-pooling processes are related through the principle of the detailed balance, i.e. $k^{\mathrm{back}}_{5\mathrm{S}} = k_{5\mathrm{S}}(g_{3\mathrm{P}}/g_{5\mathrm{S}}) \exp\{-\Delta E/(k_{\mathrm{B}}T)\}$, where $g_{3\mathrm{P}}$ and $g_{5\mathrm{S}}$ are the statistical weights of the initial (3P + 3P) and final (5S + 3S) state, respectively, and $\Delta E = 734.6\ \mathrm{cm}^{-1}$ is the energy defect for the process (1). Consequently, the back-pooling rate can be expressed as $R^{\mathrm{back}}_{5\mathrm{S}} = e_{5\mathrm{S}}k_{5\mathrm{S}}N_{3\mathrm{S}}$, where $e_{5\mathrm{S}} = (g_{3\mathrm{P}}/g_{5\mathrm{S}}) \exp\{-\Delta E/(k_{\mathrm{B}}T)\}$.

It has been proven that $\mathcal{F}_{5\mathrm{S}}(y) = \mathcal{F}^{2}_{3/2}(y)$ [18,23], and since the measured $\mathcal{F}_{3/2}(y)$ exhibited the Gaussian shape, the ratio of the integrals of the 5S and $3\mathrm{P}_{3/2}$ distributions amounts to 0.7. By combination of relations (3), (5), (7) and (8), and taking into account the above elaborations, the final expression for $k_{5\mathrm{S}}$ is

$$k_{5\mathrm{S}} \quad = \quad \frac{A_{5\mathrm{S}}\varepsilon}{1 - \varepsilon e_{5\mathrm{S}}N_{3\mathrm{S}}}, \tag{9}$$

where

$$\varepsilon \;=\; \frac{1.531\cdot 10^4}{\left(1+\eta\right)^2}\,\frac{I_{616}^{\mathrm{meas}}}{I_{3/2}^{\mathrm{meas}}(\Delta\nu)}\,\frac{N_{3\mathrm{S}}}{N_{3\mathrm{P}_{3/2}}^{c}}\,\frac{\mathcal{P}_{3/2}(\Delta\nu)}{(\Delta\nu)^2}\,\exp\{-h\Delta\nu/(k_{\mathrm{B}}T)\}. \qquad (10)$$

In the above expression, numerical values for all known quantities that appear have been substituted. In the evaluation of the results, the value $A_{5\mathrm{S}} = 1.28\cdot 10^7\ \mathrm{s}^{-1}$ given by [24] was used.

The cross section $\sigma_{5\mathrm{S}}$ for the process (1) was calculated according to

$$\sigma_{5\mathrm{S}} \;=\; \frac{k_{5\mathrm{S}}}{\overline{v}} \qquad (11)$$

using the $k_{5\mathrm{S}}$ values evaluated according to Eqs. (9) and (10), and the Maxwellian mean relative velocity $\overline{v}$ of the colliding sodium atoms determined in the way described in the previous section.

The reliability of the $\sigma_{5\mathrm{S}}$ data determined according to Eqs. (9)–(11) depends on how good does the theoretical absorption profile $\mathcal{P}_{3/2}(Y)$ reproduce the emission profile of the sodium D2 line in the blue quasistatic wing. It has been shown in Ref. [7] that the reproduction is excellent.

3. Measurement procedure and results

To determine the cross section $\sigma_{5\mathrm{S}}$ for the energy pooling process (1) according to Eqs. (9)–(11), it was necessary to measure sodium ground-state number density $N_{3\mathrm{S}}$, the fluorescence intensity I_{616} of the energy pooling line at the $5\mathrm{S}\rightarrow 3\mathrm{P}_{3/2}$ transition relative to the fluorescence intensity $I_{3/2}(\Delta\nu)$ in the optically thin region of the quasistatic wing of the D2 line, the number density of sodium atoms in the $3\mathrm{P}_{3/2}$ state, $N_{3/2}^{c}$, and their spatial distribution $N_{3/2}(r)$, the relative population η of the fine structure levels of the 3P state and the relative velocity $\overline{v}$ of the colliding sodium atoms.

The determination of the ground state sodium density and relative velocity $\overline{v}$ is explained in Sect. 2.1 and all other relevant details can be found in Ref. [7].

While exciting the sodium atoms at full pump power by the laser, which was locked at the detuning $\Delta\nu_L = \nu_{1/2} - \nu_L$ in the red wing of the D1 line, the fluorescence intensities of the sodium resonance doublet and the energy pooling lines at $5\mathrm{S}_{1/2}\rightarrow 3\mathrm{P}_{3/2}$ and $5\mathrm{S}_{1/2}\rightarrow 3\mathrm{P}_{1/2}$ transitions (616.2 and 615.6 nm) were recorded by scanning the monochromator.

It was not necessary to correct either of the measured fluorescence intensities for the absorption along the optical path d. Namely, the $3\mathrm{S}_{1/2}\rightarrow 3\mathrm{P}_{3/2}$ absorption (measured along the optical path $L \approx 4d$) was not detectable at typical wing detunings $\Delta\nu$ ($\Delta\lambda \geq 0.6$ nm) appearing in Eq. (10).

With the exciting laser still kept locked at the pump frequency ν_L, the diode laser was shone through the centre of the excitation zone and the absorption was

measured at the $3P_{3/2} \rightarrow 3D$ transition. To make the 819.7 nm line optically thin, which was necessary for correct determination of $N^c_{3/2}$, the pump power had to be substantially reduced by neutral density filters. That in turn caused the decrease of the energy pooling signal, which became undetectable. Therefore, the population density $N^c_{3/2}$ realised with the full pump power had to be calculated according to $N^c_{3/2} = \hat{N}^c_{3/2} P_0/\hat{P}$, where $\hat{N}^c_{3/2}$, created with the lowest used pump power $\hat{P}$, was obtained from the corresponding peak absorption coefficient of the 819.7 nm line. It was verified that $N^c_{3/2}$ scales linearly with the pump power by measuring the fluorescence wing intensity $I_{3/2}$ at a certain fixed detuning in the blue wing of the D2 line as a function of the applied pump power, which in the conditions of constant ground-state number density, reflects the population of the $3P_{3/2}$ state. Simultaneously, the intensity I_{616} of the energy pooling line was also measured as a function of the applied pump power, in order to check whether the applied pump powers caused any trapping of the $5S \rightarrow 3P_{3/2}$ fluorescence. The intensity I_{616} was found to vary as $I_{616} \propto \left(N^c_{3/2}\right)^2 \propto I^2_{3/2}$ as it should in the absence of the radiation trapping.

Pumping with full laser power produced typical $N^c_{3/2}$ populations in the range between $4 \cdot 10^{10}$ and $1.4 \cdot 10^{11}$ cm^{-3}, depending on the laser power and the detuning $\Delta\nu_L$ chosen for the excitation.

The spatial distribution of the sodium atoms in $3P_{3/2}$ state was determined by measuring the corresponding peak absorption at the $3P_{3/2} \rightarrow 3D_{3/2,5/2}$ transition, while the diode-laser beam (probe) was translated across the excitation zone diameter maintaining the probe beam parallel with the pump beam. The excited $3P_{3/2}$ population was found to be completely confined to the excitation zone, and its normalized distribution $\mathcal{F}_{3/2}(r)$ exhibited the Gaussian shape. This somewhat unusual effect of the spatial distribution shrinkage at high ground-state densities has already been observed previously [25]. Since it was experimentally verified that $I_{616} \propto I^2_{3/2}$, i.e. $N^c_{5S} \propto \left(N^c_{3/2}\right)^2$, the normalised distribution of the 5S atoms acquires the form $\mathcal{F}_{5S}(r) = \mathcal{F}^2_{3/2}(r)$. Consequently, the ratio of the integrals of the 5S and $3P_{3/2}$ distributions is equal to 0.7, as already anticipated in the evaluation of Eqs. (9) and (10).

The $3P_{1/2}$ to $3P_{3/2}$ population ratio η was determined from the ratio of the fluorescence intensities measured in the outer wings of the D lines, by using the Eq. (8) and analogous one for the wing of D1 line ($\mathcal{F}_{3/2}$ and $\mathcal{F}_{1/2}$ were found to be the same). From the experiment, it was found that $\eta = 0.6$, suggesting that the 3P fine-structure states were not completely mixed at the investigated temperatures. Namely, the thermodynamic value of η is equal to 0.52 at the average experimental temperature of 620 K. A similar effect was observed in sodium vapour earlier by Davidson et al. [26].

The overall error bar of the σ_{5S} includes contributions due to the uncertainties in the experimental quantities N_{3S}, $N^c_{3/2}$, $I_{3/2}$, I_{616} and $\overline{\nu}$.

The errors in the determination of N_{3S} and $N^c_{3/2}$ amount to ± 10 % and are

caused by the uncertainty of the vapour-column length determination. Both number densities were measured along the same optical path, and since they appear as the ratio in Eq. (10), the contribution to the overall error amounts to ±10 %.

At all investigated temperatures, the number densities produced in the $3P_{3/2}$ state were comparable in value, which ensured avoidance of the trapping of the 5S $\rightarrow$ $3P_{3/2}$ fluorescence, so that the 5S state was always populated at similar rates. On the other hand, the losses due to back-pooling increased proportionally to the increased N_{3S} density, causing the observed energy pooling signals to decrease. That is why the measurements were not extended to temperatures higher than reported. The highest uncertainty in the I_{616} intensity determination (high temperatures) was ±25 %.

The error bar of energy pooling signals in the present experiment is larger than in the previous similar experiment [7] dealing with energy pooling to the Na 4D state. The reason for that lies in the fact that the $3P_{3/2}$ populations in both experiments had to be comparable to avoid the radiation trapping of the monitored energy pooling lines. Since the energy pooling to the Na 5S state is less efficient than the pooling to the 4D state, the pooling signals in the present experiment were effectively weaker and have been determined with a lower accuracy than the previous ones.

The reason for not extending the measurements to temperatures lower than 567 K ($N_{3S} = 2.2 \cdot 10^{14}$ cm^{-3}) lies in the fact that the quasistatic wing at detunings $\lambda \approx 1$ nm (requirement $\Delta\lambda \gg \delta\lambda = 0.1$ nm, see text preceding Eq. (8)) was not sufficiently pronounced at lower temperatures. The intensity $I_{3/2}$ was measured with the relative error up to ±10 % (lowest temperatures).

With all sources of the uncertainties taken into account by adding errors in quadrature, the k_{5S} was determined with an overall standard error of ±30 %.

The results obtained for the energy-pooling cross section σ_{5S} as a function of temperature are shown in Fig. 2. If the back-energy pooling would not have been taken into account in the evaluation of the results, the obtained values for σ_{5S} would be between 1 % and 15 % lower than those displayed, the reduction rising progressively with the increase of the temperature.

Previously published experimental values [10,11] are also displayed in Fig. 2. Only recent theoretical calculations published in Ref. [17] are included in the figure. All earlier theoretical results [13–16] for the $\sigma_{5S}(T)$ lie too low (by a factor of 3 to 60 % at best) compared with the data displayed in Fig. 2. The present measurements show that the cross section σ_{5S} exhibits negative temperature slope, which is expected for the class of exothermic processes to which reaction (1) belongs. The inset in Fig. 2 displays $\log \sigma_{5S}$ vs. $\log T$ plot. From the linear regression through the experimental points (all available experimental data are included in the analysis) it was found that the cross section exhibits $\sigma_{5S} \propto T^{-1.3}$ dependence. The temperature exponent is determined with the accuracy of ±25 %. The declared error bar includes the statistical uncertainty of the straight line fit through the data weighted by their error bars and the uncertainty in the determination of the abscissa (T) value.

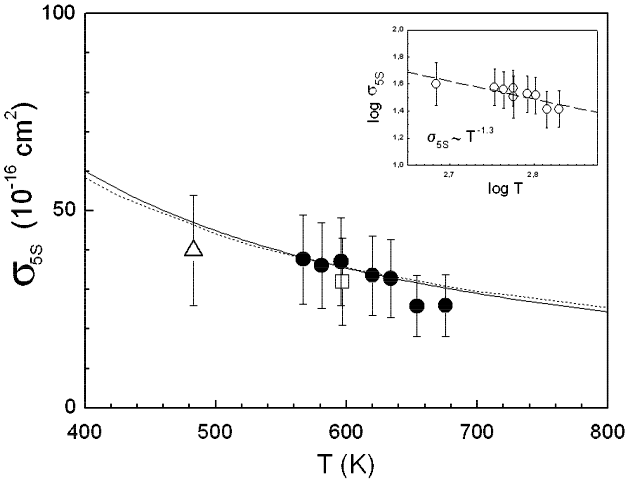

Fig. 2. The cross section σ_{5S} *for the energy pooling process* Na(3P) + Na(3P) → Na(5S) + Na(3S), *as a function of temperature. Experimental results: triangle - Allegrini et al. [11], square - Huennekens and Gallagher [10], full dots - present work. Theoretical result: dotted line - recent theoretical calculation of Yurova [17]; the curve displayed is obtained as a weighted average of the* (J, J') *- selective cross sections (data are digitised from the figures in the original paper) given in [17] to enable correct comparison with the present experiment in which the fine-structure levels of the initial* 3P *state were populated in the statistical ratio. The determination of the* σ_{5S} *temperature dependence is illustrated in the inset. All available experimental data are included in the analysis, yielding* $\sigma_{5S} \propto T^{-1.3}$ *dependence, which is indicated with full line in the picture.*

4. Discussion

As can be seen in Fig. 2, there is a very good agreement between the previously published σ_{5S} value at a single temperature $T = 600$ K [10] and the present measurements of $\sigma_{5S}(T)$ at the same temperature. Also, the result reported in Ref. [11] at $T = 483$ K agrees very well with the value that $\sigma_{5S} \propto T^{-1.3}$ dependence predicts for that temperature. Theoretical calculations published recently [17] for the $\sigma_{5S}(T)$ that account for the fine-structure effects, which are inherent to all experimental values, are in a very good agreement with the present experimental results as well. By fitting the theoretical $\sigma_{5S}(T)$ curve to $\sigma_{5S} \propto T^{-a}$ dependence, the coefficient a is obtained to be $a = 1.2$ which is within the experimental error bar of the present value.

As already mentioned in the Introduction, it is very helpful to make a systematisation of the CEET cross section with respect to a given characteristic parameter, for instance the temperature. If such systematisation would yield a certain empirically established regularity, it would be even more useful, because that could be used for the estimation of the cross sections for the processes or temperature regions that have not yet been investigated.

In the following, two regularities regarding the temperature behaviour of the CEET cross sections will be addressed. The first one concerns the cross sections for energy pooling processes to the 5S and 4D states in sodium. The other one is more general and involves various collision partners and various types of exothermic CEET processes with different energy defects.

Using the present $\sigma_{5S}(T)$ values and previously reported data for $\sigma_{4D}(T)$ [7], the temperature dependence of the σ_{4D}/σ_{5S} ratio is determined and the results (full circles) plotted against the inverse temperature are shown in Fig. 3. Both $\sigma_{4D}(T)$ and σ_{5S}(T) values have been measured in the conditions of thoroughly mixed fine-structure levels ($J = 1/2,\ 3/2$) of the sodium 3P state. Therefore the σ values comprise the contributions from all three types of the collisions regarding the J values of the atoms in the initial state, i.e. these cross sections correspond to the energy pooling produced by $(1/2, 1/2)$, $(1/2, 3/2)$ and $(3/2, 3/2)$ collisions. The results of other authors [8,26], who performed the cross-section measurements under the same conditions of statistically populated 3P fine-structure states, are also displayed in the figure, and these σ_{4D}/σ_{5S} data are labelled with open circles in Fig. 3 (numbers next to symbols denote the corresponding references). The least-squares fit through all available data (full and open circles) for the cross-section ratios

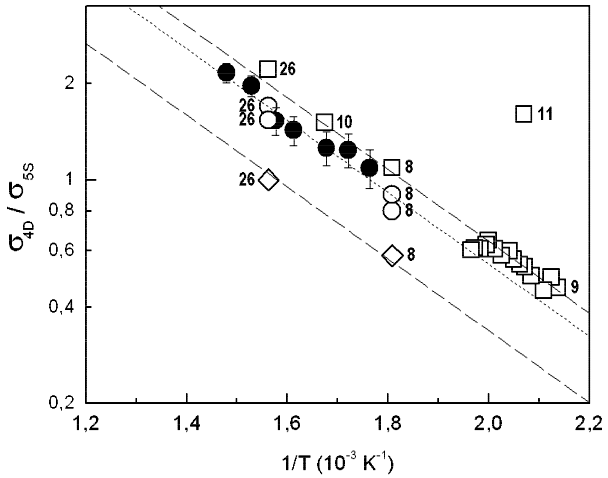

Fig. 3. Ratio of the cross sections σ_{4D}/σ_{5S} for the processes $\mathrm{Na}(3P_J) + \mathrm{Na}(3P_{J'}) \rightarrow \mathrm{Na}(4D,\ 5S) + \mathrm{Na}(3S)$ *as a function of the inverse temperature, for different initial state (J, J') combinations. Circles (full and open), correspond to the energy-pooling processes in which all three types $(1/2, 1/2)$, $(1/2, 3/2)$ of collisions are present. Results obtained in the conditions of pure $(3/2, 3/2)$ and $(1/2, 1/2)$ collisions are depicted with open squares and diamonds, respectively. Numbers next to symbols label the corresponding references. The cross-section ratios obtained using the present results for σ_{5S} and previously published ones for σ_{4D} [7] are labelled with full circles. The dotted line is a least-squares fit through all data represented with circles (full and open). The dashed lines are only guides for the eye.*

measured when $3P_J$ states are completely collisionally mixed, yielded the temperature dependence $\sigma_{4D}/\sigma_{5S} \propto \exp\{-1855/(k_B T)\}$, which is shown by the dotted line.

Figure 3 also includes the results [8-11, 26] obtained in the regime when energy pooling processes were due to pure $(3/2, 3/2)$ or $(1/2, 1/2)$ collisions, which occurred when the $3P_J$ levels were selectively excited by laser in pure sodium vapour at low ground-state densities ($\sim 10^{12}$ cm^{-3}). The data corresponding to the pure $(3/2, 3/2)$ and $(1/2, 1/2)$ collisions are represented with open squares and diamonds, respectively. The dashed lines through these data are only guides for the eye. From Fig. 3, it can be concluded that the type of the collision regime influences the absolute value of the cross-section ratio σ_{4D}/σ_{5S}, while its temperature dependence remains practically unaffected.

In the group of the results obtained for pure $(3/2, 3/2)$ collisions, the datum from Ref. [11] is in substantial disagreement with others. The cause of this discrepancy lies in the fact that σ_{4D} value obtained in Ref. [11] is too high (see discussion in Ref. [7]).

The results of measurements published in Ref. [8] were not quantitative, i.e. the authors reported only the relative intensities of the energy pooling lines 4D $\rightarrow$ 3P and 5S $\rightarrow$ 3P transitions, together with data about the temperature (Na ground-state density) and pressure of the buffer gas (Ne). However, these data were sufficient to calculate the cross-section ratios, using Eq. (9) and the analogous one for k_{4D} published previously [7], if in both equations back-pooling was neglected, which is justified at Na ground-state densities ($\approx 10^{12}$ cm^{-3}) realised in Ref. [8]. The values of σ_{4D}/σ_{5S} obtained in this way are displayed in Fig. 3.

The absolute values of the σ_{4D} and σ_{5S} cross sections obtained in Ref. [9] are several orders of magnitude smaller than the results of other authors [7,10,11, present values], due to large systematic errors in the determination of relevant quantities. However, when taking the ratio of the cross sections, all sources of errors cancel out, and, as can be seen in Fig. 3, these data fit very well in the overall picture. These measurements were made in pure Na vapour, covering the ground-state densities in the range $2{\cdot}10^{12}$ to $2{\cdot}10^{13}$ cm^{-3}. At the high-density end of the investigated interval, the collisional mixing of $3P_J$ levels starts to be important, which manifests itself in the deviation of the corresponding σ_{4D}/σ_{5S} values towards the straight line corresponding to the collision regime in which the ratio of the excited atom populations in the fine-structure states approaches thermodynamic value.

Recently [3], an interesting empirical relationship between the magnitude of the exothermic CEET cross-sections and their dependence on temperature has been published, based on the collection of data available in literature. Here, this finding is reproduced in Fig. 4 and the results of the present investigation are added. As can be seen in Fig. 4, there is a continuous change in dependence from approximately $\sigma \propto T^2$ to $\sigma \propto T^{-1.5}$ from the lowest to the highest cross-section values that span over eight orders of magnitude. No data in the cross-section databases were found that would violate the observed regularity, which applies to like and unlike collision partners and various types of CEET processes with different energy defects. This

suggests that neither the energy defect nor the type of interaction, but only the absolute magnitude of the thermal cross-sections is crucial for the thermal cross-section temperature behaviour. In particular, the cross sections of the order of magnitude of 10^{-15} cm^2 are temperature-independent (zero slope of $\sigma(T)$ in Fig. 4). It should be noted that this cross-section value is of the same order of magnitude as the geometrical cross section for the atom-atom collision in which both atoms involved are in their ground states.

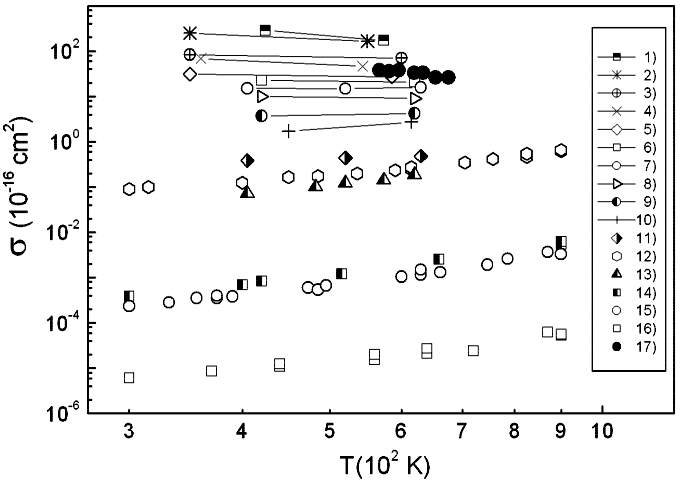

Fig. 4. The temperature dependence of the various exothermic CEET processes, showing the change of the slope of the $\sigma(T)$ curve depending on the magnitude of the exothermic cross section, which spans over eight orders of magnitude. A continuous transformation from a $\sigma(T) \propto T^2$ to a $\sigma(T) \propto T^{-1.5}$ dependence can be seen. Various collision partners and also various types of CEET processes with different energy defects are included in the figure.

1) $Na(3P_{3/2}) + Na(3S) \rightarrow Na(3P_{1/2}) + Na(3S)$ *[1,27];*
2) $K(4P_{3/2}) + K(4S) \rightarrow K(4P_{1/2}) + K(4S)$ *[1];*
3) $Cs(6P_{3/2}) + Cs(6P_{3/2}) \rightarrow Cs(6D) + Cs(6S)$ *[28,29];*
4) $Rb(5P_{3/2}) + Rb(5S) \rightarrow Rb(5P_{1/2}) + Rb(5S)$ *[1];*
5) $Cs(6P_{3/2}) + Cs(6S) \rightarrow Cs(6P_{1/2}) + Cs(6S)$ *[30,31];*
6) $Cs(8P_{3/2}) + He \rightarrow Cs(8P_{1/2}) + He$ *[32];*
7) $Cs(7P_{3/2}) + He \rightarrow Cs(7P_{1/2}) + He$ *[33];*
8) $Cs(8P_{3/2}) + Xe \rightarrow Cs(8P_{1/2}) + Xe$ *[32];*
9) $Cs(8P_{3/2}) + Ar \rightarrow Cs(8P_{1/2}) + Ar$ *[32];*
10) $Cs(6D_{3/2}) + He \rightarrow Cs(7P_{1/2}) + He$ *[34];*
11) $Cs(7P_{3/2}) + Xe \rightarrow Cs(7P_{1/2}) + Xe$ *[33];*
12) $Rb(5P_{3/2}) + He \rightarrow Rb(5P_{1/2}) + He$ *[35];*
13) $Cs(7P_{3/2}) + Ar \rightarrow Cs(7P_{1/2}) + Ar$ *[33];*
14) $Rb(5P_{3/2}) + Xe \rightarrow Rb(5P_{1/2}) + Xe$ *[35];*
15) $Cs(6P_{3/2}) + He \rightarrow Cs(6P_{1/2}) + He$ *[35];*
16) $Cs(6P_{3/2}) + Ne \rightarrow Cs(6P_{1/2}) + Ne$ *[35];*

17) present work: Na(3P) + Na(3P) → Na(5S) +Na(3S).

As can be seen, the present results on the temperature dependence of the cross section for the exothermic energy pooling process Na(3P) + Na(3P) → Na(5S) + Na(3S) fit very well in the existing field of the σ vs. T curves for exothermic CEET processes.

5. *Conclusion*

The temperature dependence of the cross section σ_{5S} for the energy pooling process Na(3P) + Na(3P) → Na(5S) + Na(3S) has been determined in the range between 567 and 676 K. The measurements have shown that the cross section decreases as the temperature increases, exhibiting the $\sigma_{5S} \propto T^{-1.3}$ dependence. Previously reported σ_{5S} value measured at $T = 600$ K [10] is in excellent agreement with the present value at the same temperature. Also, the result from Ref. [11] obtained at $T = 483$ K is in very good agreement with the value predicted by the temperature dependence reported here. Moreover, recent theoretical calculations [17] of the $\sigma_{5S}(T)$, which take into account fine-structure effects, are in very good agreement with the present experimental results. Regarding the notorious disagreement between the experimental and theoretical results when CEET cross sections are in question (theoretical values are almost always much too small when compared with the measured ones), this agreement might be even considered to be excellent.

The temperature dependence of the ratio of the cross sections for energy pooling processes to 5S and 4D states in sodium, occurring in the collisions that involve completely collisionally mixed populations in the initial $3P_J$ states, has been obtained using the present $\sigma_{5S}(T)$ results and previously [7] published ones for $\sigma_{4D}(T)$. It was found that $\sigma_{4D}/\sigma_{5S} \propto \exp\{-1855/(k_B T)\}$. By including into the consideration the results of other authors who measured these cross sections in collisions which involved pure $3P_{1/2}$ or pure $3P_{3/2}$ initial state population, it was found that the change of the collision regime did not affect the temperature dependence, but only the magnitude of the σ_{4D}/σ_{5S} ratio ($(1/2, 1/2)$ and $(3/2, 3/2)$ collisions produced the lowest and the highest cross-section ratios, respectively).

The obtained data for $\sigma_{5S}(T)$ have been found to fit very well into the field of continuously slope varying $\sigma(T)$ curves [3] for exothermic CEET processes. This regularity between the magnitude of the exothermic CEET cross section and the slope of the corresponding $\sigma(T)$ curve was recently established empirically, and the present results have been found to support its validity.

Acknowledgements

The author acknowledges the financial support by the Ministry of Science and Technology, Republic of Croatia.

References

[1] L. Krause, in *The Excited State in Chemical Physics*, ed. J. W. McGowan, Wiley, New York (1975) p. 267.

[2] W. Demtröder, *Laser Spectroscopy*, Springer Verlag, Berlin (1995).

[3] C. Vadla, V. Horvatić and K. Niemax, Spectrochimica Acta B **58** (2003) 1235.

[4] A. Ekers, M. Glodz, V. Grushevsky, J. Kalvins and J. Szonert, Can. J. Phys. **79** (2001) 1039.

[5] A. Gallagher, Phys. Rev. **172** (1968) 88.

[6] I. N. Siara, H. S. Kwong and L. Krause, Can. J. Phys. **52** (1974) 945.

[7] V. Horvatić, M. Movre and C. Vadla, J. Phys. B: At. Mol. Opt. Phys. **32** (1999) 4957.

[8] M. Allegrini, G. Alzetta, A. Kopystynska and L. Moi, Opt. Commun. **19** (1976) 96.

[9] V. S. Kushawaha and J. J. Levental, Phys. Rev. A **25** (1982) 570.

[10] J. Huennekens and A. Gallagher, Phys. Rev. A **27** (1983) 771.

[11] M. Allegrini, P. Bicchi and L. Moi, Phys. Rev. A **28** (1983) 1338.

[12] N. N Bezuglov, A. N Klucharev and V. A. M. Sheverev, J. Phys. B: At. Mol. Phys. **20** (1987) 2497.

[13] P. Kowalczyk, J. Phys. B: At. Mol. Phys. **17** (1984) 817.

[14] S. Geltman, Phys. Rev. A **40** (1989) 2301.

[15] P. H. T. Philipsen, J. H. Nijland, H. Rudolph and H. G. M. Heideman, J. Phys. B: At. Mol. Phys. **26** (1993) 939.

[16] I. Yu. Yurova, O. Dulieu, S. Magnier, F. Masnou-Seeuws and V. N. Ostrovskii, J. Phys. B: At. Mol. Phys. **27** (1994) 3659.

[17] I. Yu. Yurova, Phys. Rev. A **65** (2002) 032726.

[18] C. Vadla, K. Niemax and J. Brust, Z. Phys. D **37** (1996) 241.

[19] V. Horvatić, M. Movre, R. Beuc and C. Vadla, J. Phys. B: At. Mol. Phys. **26** (1993) 3679.

[20] A. N. Nesmeyanov, *Vapour Pressure of the Elements*, Academic Press, New York (1963).

[21] W. L. Wiese, M. W. Smith and B. M. Miles, *Atomic Transition Probabilities (NSRDS-NBS 22)*, Vol 2, Washington, US Govt Printing Office (1969).

[22] M. Movre and G. Pichler, J. Phys. B: At. Mol. Phys. **13** (1980) 697.

[23] C. Vadla, K. Niemax and V. Horvatić, Eur. Phys. J. D **1** (1998) 139.

[24] W. Hansen, J. Phys. B: At. Mol. Opt. Phys. **17** (1984) 4833.

[25] T. Scholz, M. Schiffer, J. Welzel, D. Cysarz and W. Lange, Phys. Rev. A **53** (1996) 2169.

[26] S. A. Davidson, J. F. Kelly and A. Gallagher, Phys. Rev. A **33** (1986) 3756.

[27] J. Huennekens and A. Gallagher, Phys. Rev. A **27** (1983) 1851.

[28] C. Vadla, Eur. Phys. J. D **1** (1998) 259.

[29] Z. J. Jabbour, R. K. Namiotka, J. Huennekens, M. Allegrini, S. Milošević and F. de Tomasi, Phys. Rev. A **54** (1996) 1372.

[30] M. Czajkowski and L. Krause, Can. J. Phys. **43** (1965) 1259.

[31] M. Movre, V. Horvatić and C. Vadla, J. Phys. B: At. Mol. Opt. Phys. **32** (1999) 4647.

[32] M. Pimbert, J. Physique **33** (1972) 331.

[33] I. N. Siara, H. S. Kwong and L. Krause, Can. J. Phys. **52** (1974) 945.

[34] J. Cuvellier, P. R. Fournier, F. Gounand, J. Pascale and J. Berlande, Phys. Rev. A **11** (1975) 846.

[35] A. Gallagher, Phys. Rev. **172** (1968) 88.

TEMPERATURNA OVISNOST UDARNOG PRESJEKA σ_{5S} ZA PROCES ENERGIJSKOG ZDRUŽIVANJA Na(3P) + Na(3P) → Na(5S) + Na(3S)

Primjenom metode laserski inducirane fluorescencije određen je udarni presjek σ_{5S} za proces združivanja energije (engl. energy pooling process) Na(3P) + Na(3P) → Na(5S) + Na(3S) u temperaturnom području od 567 to 676 K. Ustanovljeno je da se vrijednosti za σ_{5S} smanjuju s porastom temperature, pri čemu se pokazuje ovisnost $\sigma_{5S} \propto T^{-1.3}$. Dobiveni rezultati se izvrsno slažu s najnovijim teorijskim računima. Također, pokazano je da se mjerena temperaturna ovisnost udarnog presjeka σ_{5S} vrlo dobro uklapa u opću sliku ovisnosti između σ i T, što je bila nedavno objavljena, a uključuje različite sudarne partnere i različite vrste sudarnih prijenosa energije pobude s različitim energijskim defektima.